

Cite this: *Org. Chem. Res.* **2022**, *8*, 9-15.

DOI: 10.22036/org.chem.2023.401924.1288

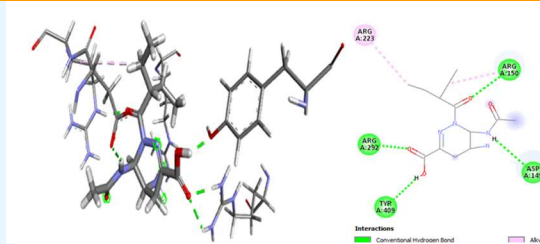
Molecular Docking Study of the Inhibition Influenza B Virus by Some Selected Carboxylic Acids

David Ebuka Arthur*, Ayuba Maina, Aroh Augustina Oyibo, Haruna Bulama Wayar, Sule Ibrahim, Hadiza Adamu Dawi

Department of Pure and Applied Chemistry, University of Maiduguri, Nigeria. E-mail: eadavid@unimaid.edu.ng

Received: January 1, 2023; Accepted: June 1, 2023

Abstract: Influenza viruses are major human pathogens responsible for respiratory diseases affecting millions of people worldwide and are characterized by high morbidity and significant mortality. Influenza infections can be controlled by vaccination and antiviral drugs. A molecular docking study was conducted to compute the scoring function and research protein-ligand interactions in predicting the binding affinity and biochemical activity of some carboxylic acids compounds (6-acetamido-5-amino-1-(2-ethylbutanoyl)-1,4,5,6-tetrahydropyridazine-3-carboxylic acid; 6-acetamido-5-((diaminomethylene)amino)-1-(2-ethylbutanoyl)-1,4,5,6-tetrahydropyridazine-3-carboxylic acid; 5-amino-1-(2-ethylbutanoyl)-6-((fluorocarbonyl)amino)-1,4,5,6-tetrahydropyridazine-3-carboxylic acid). The docking results show that THP3b (5-amino-1-(2ethylbutanoyl)-6-((fluorocarbonyl)amino)-1,4,5,6-tetrahydropyridazine-3-carboxylic acid) has the lowest binding affinity with a score of -19.244 kcal/mol but, in turn, has the best binding affinity when compared to all other compounds. The result confirms that the designed ligand THP3b is very stable and maintains its firm position within the binding pocket of I1NF receptor, indicating that the complex is stable under the varying conditions and THP3b can be used as a drug candidate for treating influenza B virus.

**Keywords:** Molecular docking, Influenza B, I1NF receptor, Ligand

1. Introduction

Influenza B viruses are recognized as significant respiratory pathogens, causing substantial illness, death, and economic losses during annual epidemics. Belonging to the Orthomyxoviridae family, these viruses possess a negative-sense, segmented RNA genome and are enveloped, single-stranded RNA viruses with helical symmetry, measuring approximately 80-120 nm in diameter. The nucleoprotein tightly associates with RNA to form a helical structure, and the virus consists of four antigens: haemagglutinin (HA), neuraminidase (NA), nucleocapsid (NA), and matrix (M).¹ Among these antigens, nucleoprotein (NP) is crucial in categorizing human influenza viruses into three types: A, B, and C.^{2,3}

The matrix protein (M) plays a vital role in encapsulating the nucleocapsid, constituting 35-45% of the total viral particle mass. On the viral envelope, two surface glycoproteins, haemagglutinin (HA) and neuraminidase (NA), are observed as rod-shaped projections.⁴ HA, composed of two subunits (HA1 and HA2), facilitates the virus's attachment to the cellular receptor, while NA molecules are present in lower quantities on the viral surface.⁵

It is essential to differentiate influenza from the stomach "flu" viruses that cause gastrointestinal symptoms like diarrhea and

vomiting. Influenza, commonly referred to as the flu, can be a severe illness, particularly for certain high-risk groups, such as young children under 5 (especially those under 6 months), adults over 65, individuals in long-term care facilities, pregnant women, individuals with weakened immune systems, native Americans, and those with chronic medical conditions such as asthma, heart disease, kidney disease, liver disease, diabetes, and severe obesity (Body mass index of 40 or higher).^{6,7}

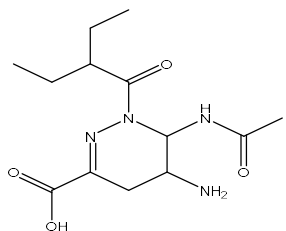
Preventive measures, especially the annual flu vaccine, are crucial in defending against the flu, even though it may not provide 100% protection. In recent years, the use of computational methods, like Pyrex and Discovery Studio Schrodinger Suite, in drug design and discovery has gained popularity due to advancements in drug discovery knowledge and increased computer power.^{8,9} These methods offer potential benefits in reducing the cost, time, and complexity associated with the drug discovery and development process for influenza B virus. Moreover, they promote green chemistry and decrease reliance on lengthy and expensive animal testing, thereby enhancing efficiency while minimizing chemical waste.¹⁰ In line with the article's title, this research holds significant importance in exploring potential inhibitory agents using computational docking

techniques, which could lead to the development of novel and effective treatments against influenza B virus infections.^{11,12}

2. Experimental

Materials and method

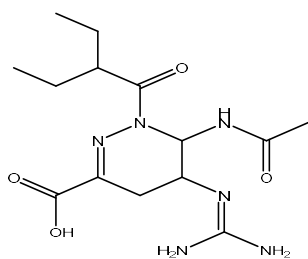
Experiment data sets and ligand preparation. Figures 1 to 3 show the chemical structures of the ligand and their corresponding IUPAC names. ChemDraw software ultra-version 12.0¹³ was used to draw the 2D structures of the natural products that have activity against influenza B virus. The compounds were collected from bindingdb database (http://www.bindingdb.org/jsp/dbsearch/PrimarySearch_ki.jsp?energyterm=kJ/mole&tag=pol&polymerid=754&target=Neuraminidase+B&column=ki&startPg=0&Increment=50&submit=Search). These compounds were synthesized and experimentally evaluated by Zhang and his research team in 1999.¹⁴



6-acetamido-5-amino-1-(2-ethylbutanoyl)-1,4,5,6-tetrahydropyridazine-3-carboxylic acid

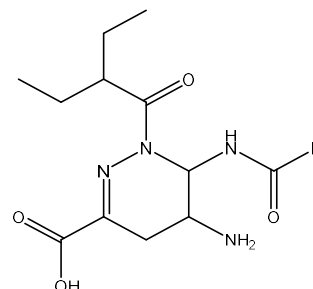
Figure 1. 2D structure of the first ligand (THP1) with its IUPAC name used in the study.

The highly functionalized ring system was assembled via a hetero Diels-Alder reaction¹⁵ of heterodiene and alkene. The structures were later used as lead templates for designing novel compounds with better activity or binding score. The chemical structure of each derivative was drawn and presented in supplementary Table1 and submitted as a supplementary file along with the manuscript. The chemical structures were assigned an alphabet starting from a to f for each lead template or compound (THP1, THP2, and THP3). These 2D structures were then transformed into 3D structures with the assistance of Spartan 14 software.¹⁶ The optimized 3D structures were generated, optimized using the DFT/B3LYP/6-311++G* level of basis set¹⁷ within the Spartan 14 software package from Wave function Inc., and saved in the pdb format for molecular docking simulations.¹⁸



6-acetamido-5-((diaminomethylene)amino)-1-(2-ethylbutanoyl)-1,4,5,6-tetrahydropyridazine-3-carboxylic acid

Figure 2. 2D structure of the second ligand (THP2) with its IUPAC name used in the study.



5-amino-1-(2-ethylbutanoyl)-6-((fluorocarbonyl)amino)-1,4,5,6-tetrahydropyridazine-3-carboxylic acid

Figure 3. 2D structure of the third ligand (THP3) with its IUPAC name used in the study.

Retrieval of receptor and preparation show. The receptor was prepared by downloading the 3D structure of the influenza virus B receptor complex (PDB: 1INF) from the Protein Data Bank.¹⁹ AutoDock MGL Tools program was used for further receptor preparation. The heteroatoms and water molecules of the receptor were manually removed from the downloaded 3D structure of the amino acid, and then saved in pdb file format.

Gibb's free energy calculations and virtual screening. A molecular interaction study was conducted to investigate the protein-ligand interactions in predicting the binding affinity and biochemical activity of the ligand.^{20,21} To estimate the binding affinity, AutoDock Vina²² 4.2 of PyRx software was used; the visualization of protein-ligand interactions including non-bonding and hydrophobic interactions was explored using the version 2016 of Discovery Studio Visualizer software.²³ The protein (PDB ID: 1INF) structure was opened in pdb format using the virtual screening instrument PyRx. For the neuraminidase model, Kollman charges and all the polar hydrogen atoms were added and file as saved to a pdb file. THP1, THP2, and THP3 were docked after covering the catalytic site of NA with a grid box of 50(x)×51(y)×47(z), grid size of 0.5 Å and centered at -2.6(x)×-5.06(y)×13.6(z). The other parameters were carried out at their default settings. The docking was achieved using Auto Dock Vina to assess the accuracy of the docking situation.

The outcomes of the work were assessed by analyzing the ligand-protein interactions, the free energy of binding, and the root mean square deviation (RMSD) values.

3. Results and Discussion

The molecular docking score for all the studied ligands is presented in Table 1 that also displays the contributions of other significant terms such as hydrogen bond energy, hydrophobic bond energy, and van der Waals interactions made by the ligands in the binding pocket of the receptor.

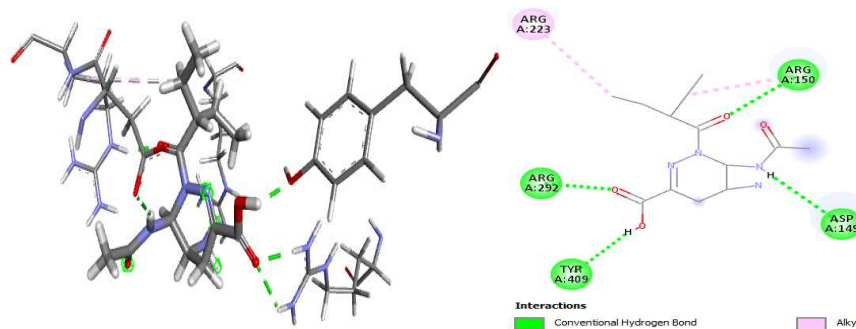
Table 1. Quantitative description of the interaction of THP1, THP2, THP3, and their analogues on IBV receptor (PDB ID: 1INF)

Name	Docking Score	Nflex	Hbond	Hphob	Vwint	Eintl	Dsolv	SolEI
THP1	8.079	8	-6.998	-4.610	-17.305	10.474	22.340	37.307
THP1a	0.350	9	-7.080	-3.631	-20.582	9.504	27.402	23.219
THP1b	-6.822	11	-11.550	-2.174	-18.940	3.248	25.171	26.240
THP1c	-9.846	12	-11.272	-2.017	-18.668	11.122	25.470	18.770
THP1d	-5.726	12	-10.443	-1.849	-15.336	6.593	26.183	15.805
THP1e	-5.540	12	-10.149	-1.543	-21.594	8.132	28.533	21.462
THP1f	-3.818	13	-7.687	-1.746	-25.090	9.766	25.864	22.263
THP1g	0.203	12	-12.120	-1.762	-21.975	6.443	31.357	35.309
THP2	-12.923	8	-13.408	-3.677	-21.562	8.788	25.846	31.576
THP2a	-6.983	8	-10.543	-3.399	-21.002	11.535	27.949	26.073
THP2b	-12.608	8	-9.318	-2.917	-22.871	9.881	21.769	22.221
THP2c	-14.043	9	-10.033	-3.303	-23.983	7.887	26.075	19.062
THP2d	-13.312	10	-9.526	-2.507	-22.809	7.093	21.783	19.604
THP2e	-4.689	9	-15.043	-1.674	-18.767	10.496	35.240	32.467
THP2f	-13.702	9	-10.669	-1.806	-23.788	8.275	29.759	16.012
THP3	0.570	8	-7.287	-3.793	-18.867	8.571	26.108	24.294
THP3a	7.436	9	-3.910	-3.816	-19.781	6.352	19.981	29.211
THP3b	-19.244	10	-13.900	-1.940	-18.898	5.018	26.360	15.684
THP3c	-3.993	10	-9.914	-2.805	-25.911	12.937	27.123	34.149
THP3d	-3.382	10	-10.281	-2.467	-26.458	11.840	28.721	35.150
THP3e	-14.461	10	-11.730	-2.117	-19.561	6.009	28.177	13.732
THP3f	-14.2403	10	-12.0978	-1.8455	-18.5799	8.48275	27.2635	14.7512

Nflex: - Number of rotatable torsions. Hbond: - hydrogen bond energy. Hphob: - hydrophobic energy in exposing a surface to water Vwint: - The van der Waals interaction energy (sum of gc and gh van der Waals). Eintl: - Internal conformational energy of the ligand. Dsolv: - The desolvation of exposed Hbond donors and acceptors. SolEI: - The solvation electrostatics energy change upon binding.

In 2021, Kumar and coworkers performed an in silico molecular docking of Berberine–Benzothiazole and Oseltamivir towards influenza B viral neuraminidase with the receptor (4WA4) and the binding energy values were found to be -8.4 kcal/mol and -6.1 kcal/mol, respectively.²⁴ By comparison, the results of the molecular docking study of 1INF receptor, Table 1, shows that THP3b and THP3e have the least binding energy of -19.244 kcal/mol and -14.461 kcal/mol, respectively. The binding poses of ligand THP1 and

THP1a presented in Figures 4 and 5, respectively, demonstrate that the ligands are perfectly placed in the binding pocket. Therefore, these binding energies are deemed favorable for docking and inhibition of IBV, indicating that THP3b and THP3e are more acceptable inhibitors of IBV than Berberine–Benzothiazole and Oseltamivir reported recently.²⁴ The amino acids are shown in two different colors. The green color shows the conventional hydrogen bonds and the lighter purple shows the Alkyl.

**Figure 4.** The 2D and 3D views of interaction types of THP1 with surrounding amino acids of 1INF.**Table 2.** Interaction types and amino acids involved in the inhibition of IBV receptor (PDB ID: 1INF) with THP1 Inhibitor

Distance (Å)	Types	From	From chemistry	To	To chemistry
1.8	Conventional hydrogen bond	A:ARG150:HE	H-Donor	THP1:O1	H-Acceptor
2.15	Conventional hydrogen bond	A:ARG292:HH12	H-Donor	THP1:O3	H-Acceptor
1.81	Conventional hydrogen bond	A:ARG292:HH22	H-Donor	THP1:O3	H-Acceptor
2.22	Conventional hydrogen bond	:THP1:H16	H-Donor	A:ASP149:OD2	H-Acceptor
1.98	Conventional hydrogen bond	:THP1:H22	H-Donor	A:TYR409:OH	H-Acceptor
4.36	Alkyl	:THP1:C10	Alkyl	A:ARG223	Alkyl
5.03	Alkyl	THP1:C7	Alkyl	A:ARG150	Alkyl

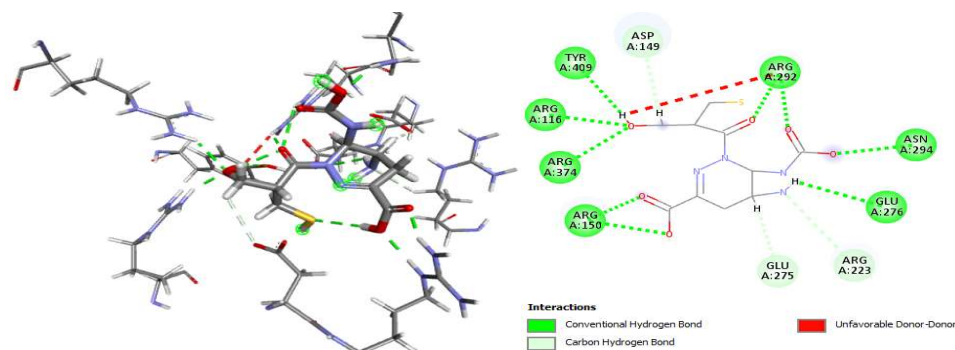


Figure 5. 2D and 3D views of interaction type of THP1a with surrounding amino acids of 1INF.

The type of bond formed at a distance of 1.8, 2.15, 1.81, 2.22, 1.98, 4.36, and 5.03 Å is a conventional hydrogen bond found donated from the H-donor of THP1:O1, THP1:O3, and THP1:O3 to the H-Acceptor of A:ASP149:OD2 in the chain of the receptor. At a distance of 4.36, an alkyl bond is formed, donated from THP1:C10 of A:ARG223. The binding score and hydrogen bond of THP1, which are responsible for the addition of interaction energy, are indicated in Table 1 (8.079 kcal/mol and -0.668 kcal/mol, respectively). This interaction is further illustrated in Table 2. Other stabilizing energies associated with the binding affinity of THP1 are linked to alkyl interactions of the ligands with the hydrogen bond interaction within the complex²⁵. The findings of this study are comparable to Ahmad et al. study in 2016, where they conducted a molecular docking investigation on the three-

dimensional model of the influenza virus nucleoprotein obtained from the Protein Data Bank (PDB ID: 3R05). Ahmad et al. employed the AMBER99 force field option of MOE to optimize the receptor molecule through energy minimization and 3D protonation. Their molecular docking results for Nimbaflavone and Rutin within the receptor binding pocket revealed the formation of hydrogen bonds between the ligands and four specific amino acids (ARG305, TYR289, TYR52, and ASP302) within the docking space. The reported docking scores for Nimbaflavone and rutin were -32.03 kcal/mol and -31.26 kcal/mol, respectively.²⁶ The amino acids are depicted in three distinct colors: green representing the traditional hydrogen bonds, sky blue signifying the carbon hydrogen bond, and red symbolizing the unfavorable donor-donor interactions.

Table 3. Interaction types and amino acids involved in the inhibition of IBV receptor (PDB ID: 1INF) with THP1a Inhibitor

Distance (Å)	Types	From	From chemistry	To	To chemistry
1.95	Conventional Hydrogen Bond	A:ARG116:HH22	H-Donor	:THP1a:O2	H-Acceptor
1.99	Conventional Hydrogen Bond	A:ARG150:HE	H-Donor	:THP1a:O6	H-Acceptor
1.66	Conventional Hydrogen Bond	A:ARG150:HH21	H-Donor	:THP1a:O5	H-Acceptor
2.52	Conventional Hydrogen Bond	A:ARG292:HH12	H-Donor	:THP1a:O1	H-Acceptor
1.63	Conventional Hydrogen Bond	A:ARG292:HH12	H-Donor	:THP1a:O4	H-Acceptor
1.72	Conventional Hydrogen Bond	A:ARG292:HH22	H-Donor	:THP1a:O1	H-Acceptor
1.93	Conventional Hydrogen Bond	A:ASN294:HD21	H-Donor	:THP1a:O3	H-Acceptor
2.19	Conventional Hydrogen Bond	A:ARG374:HH22	H-Donor	:THP1a:O2	H-Acceptor
2.09	Conventional Hydrogen Bond	:THP1a:H11	H-Donor	A:TYR409:OH	H-Acceptor
2.01	Conventional Hydrogen Bond	:THP1a:H11	H-Donor	:THP1a:O1	H-Acceptor
3.01	Conventional Hydrogen Bond	:THP1a:H13	H-Donor	A:GLU276:OE2	H-Acceptor
2.61	Conventional Hydrogen Bond	:THP1a:H16	H-Donor	:THP1a:S1	H-Acceptor
2.93	Carbon Hydrogen Bond	A:ARG223:HD1	H-Donor	:THP1a:N4	H-Acceptor
2.54	Carbon Hydrogen Bond	:THP1a:H3	H-Donor	A:GLU275:OE1	H-Acceptor
2.83	Carbon Hydrogen Bond	:THP1a:H9	H-Donor	A:ASP149:OD1	H-Acceptor

Table 3 shows the results of the interaction type and the amino acids involved between the ligand (THP1a) and the IBV receptor with the PDB ID of 1INF. The conventional hydrogen bond formed between the ligand and some amino acids is shown in the table, which is donated from A:ARG374:HH2 in chain THP1a:O1 of the receptor. Additionally, a carbon-hydrogen bond was found at a distance of 2.93 Å, donated from the amine group of THP1a:H3 in chain A:ASP165:OE1 of the receptor to the H-acceptor of the THP1a. Furthermore, a p-donor hydrogen bond was found at

The binding affinity of THP1a was primarily driven by the binding score and hydrogen bond interactions, as presented in Table 1 (6.900 kcal/mol and -2.668 kcal/mol). The presence of conventional hydrogen bonds between the ligands and the binding score of the receptor, as seen in Table 2, are the key in contributing to the overall interaction energy. Additionally, other stabilizing energy associated with the binding affinity of THP1a was attributed to hydrogen bond interactions as well as hydrogen interactions within the complex.

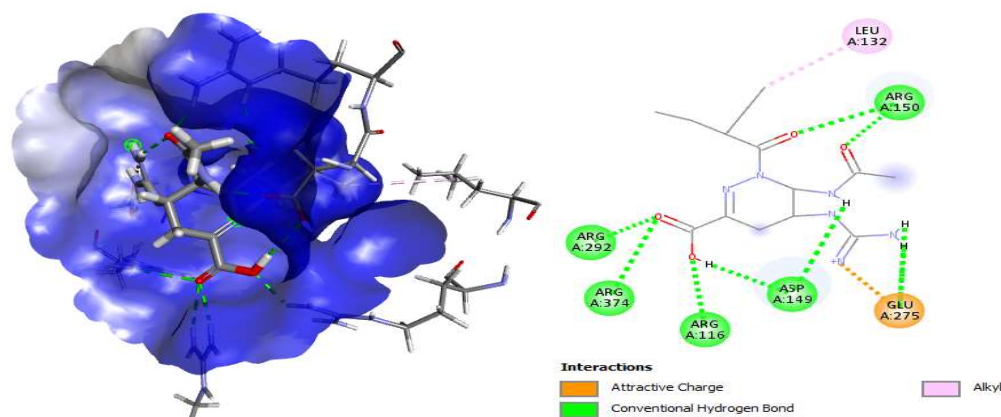


Figure 6. 2D and 3D views of interaction type of THP2 with surrounding amino acids of IINF receptor.

The green color indicates conventional hydrogen bonds, orange color indicates attractive charge, and pink color indicates alkyl between amino acids. Table 4 shows the results of the interaction types and the amino acids involved between the ligand (THP2) and the IVB receptor with the PDB ID of IINF. Four conventional hydrogen bonds form an interaction with THP2:O4 at a distance of 4.49 Å, with an attractive charge donated from negative (:THP2:N6) to the negative side of the amino acid residue (Figure 6).

Table 1 indicates that the binding score and hydrogen bond of THP2 are -9.846 kcal/mol and -11.722 kcal/mol, respectively. The conventional hydrogen bond interactions between the ligands and the receptor are primarily responsible for the binding score of the complex, which is shown in Table 1. Furthermore, the stabilizing energy associated with the

binding affinity of THP2 is linked to carbon hydrogen bond interactions with the attractive charge within the complex.

Liu and colleagues utilized AutoDock software to conduct molecular docking experiments. They employed a graphical user interface program to set up AutoDock and prepare the docking procedure. The grid box volume was established at $60 \times 50 \times 60$ with a default spacing of 0.375 Å, and they performed 100 docking runs. In their study, they used neuraminidase (4MWQ) structures as receptor for docking with small molecules like oseltamivir carboxylate, quercetin, and chlorogenic acid. The resulting docking scores for these molecules were found to be -9.38 kcal/mol, -9.41 kcal/mol, and -12.23 kcal/mol, respectively.⁸

Table 4. Interaction types and amino acids involved in the inhibition of IBV receptor (PDB ID: IINF) with THP2 Inhibitor

Distance (Å)	Types	From	From chemistry	To	To chemistry
4.49	Attractive Charge	:THP2:N6	Positive	A:GLU275:OE1	Negative
2.06	Conventional Hydrogen Bond	A:ARG116:HH22	H-Donor	:THP2:O4	H-Acceptor
2.76	Conventional Hydrogen Bond	A:ARG150:HE	H-Donor	:THP2:O1	H-Acceptor
1.64	Conventional Hydrogen Bond	A:ARG150:HH21	H-Donor	:THP2:O2	H-Acceptor
2.96	Conventional Hydrogen Bond	A:ARG292:HH12	H-Donor	:THP2:O3	H-Acceptor
1.91	Conventional Hydrogen Bond	A:ARG292:HH22	H-Donor	:THP2:O3	H-Acceptor
2.72	Conventional Hydrogen Bond	A:ARG374:HH12	H-Donor	:THP2:O3	H-Acceptor
2.33	Conventional Hydrogen Bond	A:ARG374:HH22	H-Donor	:THP2:O3	H-Acceptor
1.72	Conventional Hydrogen Bond	:THP2:H16	H-Donor	A:ASP149:OD2	H-Acceptor
2.11	Conventional Hydrogen Bond	:THP2:H20	H-Donor	A:GLU275:OE1	H-Acceptor
2.00	Conventional Hydrogen Bond	:THP2:H21	H-Donor	A:GLU275:OE2	H-Acceptor
2.46	Conventional Hydrogen Bond	:THP2:H23	H-Donor	:THP2:O2	H-Acceptor
2.70	Conventional Hydrogen Bond	:THP2:H24	H-Donor	A:ASP149:OD1	H-Acceptor
5.08	Alkyl	:THP2:C10	Alkyl	A:LEU132	Alkyl

The ligands and specific amino acids, including ASP-151, ARG-152, ARG-224, ARG-292, ASN-294, ASN-346, ARG-371, and TYR-406, were observed by the researchers to form hydrogen bonds. The docking scores obtained for THP1, THP2, and THP3 were consistent with this finding, indicating a significant similarity in the interactions responsible for the formation of the ligand-receptor complex.

The amino acids are shown in four different colors, the light green color shows the conventional hydrogen bond, the pale

green shows the carbon hydrogen bond, the orange shows salt bridge, and the purple shows the attractive charge.

The docking results of ligand THP3 and THP3b are presented in Tables 6 and 7, respectively. The ligand THP3b exhibits a significant binding affinity compared to the parent compound THP3. The number of significant conventional hydrogen bonds formed by the modified structure of THP3 is a clear indication of this. Figures 8 and 9 clearly demonstrate the distinction in interactions.

Table 5. Interaction types and amino acids involved in the inhibition of IBV receptor (PDB ID: 1INF) with THP2c Inhibitor

Distance (Å)	Types	From	From chemistry	To	To chemistry
2.12	Salt Bridge; Attractive Charge	:THP2c:H15	H-Donor;Positive	A:GLU275:OE2	H-Acceptor;Negative
4.87	Attractive Charge	:THP2c:N6	Positive	A:GLU276:OE2	Negative
1.58	Conventional Hydrogen Bond	A:ARG150:HE	H-Donor	:THP2c:O1	H-Acceptor
2.97	Conventional Hydrogen Bond	A:ARG150:HH21	H-Donor	:THP2c:O1	H-Acceptor
2.26	Conventional Hydrogen Bond	A:ARG150:HH21	H-Donor	:THP2c:N1	H-Acceptor
2.78	Conventional Hydrogen Bond	A:ARG292:HH12	H-Donor	:THP2c:O4	H-Acceptor
2.40	Conventional Hydrogen Bond	A:ARG292:HH22	H-Donor	:THP2c:O4	H-Acceptor
2.26	Conventional Hydrogen Bond	:THP2c:H10	H-Donor	A:TRP177:O	H-Acceptor
2.28	Conventional Hydrogen Bond	:THP2c:H11	H-Donor	A:ASP149:OD2	H-Acceptor
2.11	Conventional Hydrogen Bond	:THP2c:H16	H-Donor	:THP2c:O4	H-Acceptor
2.01	Conventional Hydrogen Bond	:THP2c:H17	H-Donor	A:GLU275:OE1	H-Acceptor
2.49	Carbon Hydrogen Bond	:THP2c:H7	H-Donor	A:GLU276:OE2	H-Acceptor

Table 6. Interaction types and amino acids involved in the inhibition of IBV receptor (PDB ID: 1INF) with THP3 Inhibitor

Distance (Å)	Types	From	From chemistry	To	To chemistry
1.85	Conventional Hydrogen Bond	A:ARG116:HH22	H-Donor	:THP3:O2	H-Acceptor
1.67	Conventional Hydrogen Bond	A:ARG150:HH21	H-Donor	:THP3:O4	H-Acceptor
2.56	Conventional Hydrogen Bond	A:ARG292:HH12	H-Donor	:THP3:N4	H-Acceptor
2.51	Conventional Hydrogen Bond	A:ARG374:HH22	H-Donor	:THP3:O2	H-Acceptor
2.15	Conventional Hydrogen Bond	:THP3:H16	H-Donor	A:ASP149:OD2	H-Acceptor
2.02	Conventional Hydrogen Bond	:THP3:H19	H-Donor	A:GLU117:OE2	H-Acceptor
4.29	Alkyl	:THP3:C10	Alkyl	A:ARG150	Alkyl
4.91	Pi-Alkyl	A:TRP177	Pi-Orbitals	:THP3:C10	Alkyl

Table 7. Interaction types and amino acids involved in the inhibition of IBV receptor (PDB ID: 1INF) with THP3b Inhibitor

Distance (Å)	Types	From	From chemistry	To	To chemistry
2.07	Conventional Hydrogen Bond	A:ARG116:HH22	H-Donor	:THP3b:O3	H-Acceptor
3.02	Conventional Hydrogen Bond	A:ARG150:HE	H-Donor	:THP3b:O5	H-Acceptor
1.84	Conventional Hydrogen Bond	A:ARG150:HH21	H-Donor	:THP3b:O5	H-Acceptor
2.47	Conventional Hydrogen Bond	A:ASN294:HD21	H-Donor	:THP3b:O1	H-Acceptor
2.38	Conventional Hydrogen Bond	A:GLY347:HN	H-Donor	:THP3b:O2	H-Acceptor
2.35	Conventional Hydrogen Bond	A:ARG374:HH22	H-Donor	:THP3b:O3	H-Acceptor
2.33	Conventional Hydrogen Bond	:THP3b:H12	H-Donor	A:GLU276:OE2	H-Acceptor
2.28	Conventional Hydrogen Bond	:THP3b:H13	H-Donor	A:GLU275:OE2	H-Acceptor
2.34	Conventional Hydrogen Bond	:THP3b:H14	H-Donor	A:GLU117:OE2	H-Acceptor
2.05	Conventional Hydrogen Bond	:THP3b:H8	H-Donor	A:ASN294:OD1	H-Acceptor
2.98	Halogen (Fluorine)	:THP3b:N1	Halogen Acceptor	:THP3b:F1	Halogen

4. Conclusions

In this study, three different pyridazine-3-carboxylic acid molecules were used to study the molecular interaction of these compounds with influenza virus B receptor complex (PDB: 1INF) to investigate the binding affinities of the three compounds, after which their structures were modified with the aim of improving their activity in the binding pocket. The findings indicate that ligand 2 had the best binding affinity with a score of -12.923 kcal/mol. The molecular docking results of the other compounds, designed from the three selected inhibitors, show that THP2e and THP3b had the best docking scores from the rest when we compare their hydrogen bond contributions, which in their case were presented as -15.043 kcal/mol and -13.900 kcal/mol, respectively. The hydrogen bond contribution is significant to the conformational changes that arises as a result effect of the binding affinity of a ligand, as it is known that binding energies reflect the binding affinity. However, along with binding energies, several other physical effects like electrostatic, van der

Waals forces, hydrogen bond, and hydrophobic and entropic effects influence the binding affinity that are also needed to be evaluated for calculating binding affinity of ligands or drug candidates.




Declaration of Interests

The authors declare that they have no known competing financial interests or personal relationships that could have appeared to influence the work reported in this paper.

Author Contributions

David Ebuka Arthur and Hadiza Adamu Dawi: Investigation, Methodology, Data curation, Writing-Original draft preparation. Aroh Agustina Oyibo: Supervision, Conceptualization, Writing, Reviewing and Editing. Sule Ibrahim and Ayuba Maina: Writing Reviewing and Editing, Visualization. David Ebuka Arthur and Haruna Bulama Wayar: Writing-Original draft preparation, Validation.

Author(s) ID

David Ebuka Arthur:  0000-0001-8564-868X
Hadiza Adamu Dawi:  0000-0002-8294-4173
Haruna Bulama Wayar:  0009-0000-9843-2458
Aroh Agustina Oyibo:  0009-0005-2668-2788

Acknowledgements

We express our sincere gratitude to Professor Inna A. Fanna, Professor Joseph C. Akan, and Dr. Mustapha Tijjani, who serve as pillars of support during our research journey within the Department of Pure and Applied Chemistry at the University of Maiduguri, Nigeria. We trust that their unwavering dedication to science will continue to inspire and guide fellow researchers. Our heartfelt thanks to each of them.

References

1. M. Enami, K. Enami, *J. Virol.* **1996**, *70*, 6653-6657.
2. D. R. Hijano, G. Maron, R. T. Hayden, *Front. Microbiol.* **2018**, *9*, 3097.
3. H. W. Wilkinson, R. Eagon, *Infec. Immun.* **1971**, *4*, 596-604.
4. Y. Fujiyoshi, N. P. Kume, K. Sakata, S. Sato, *EMBO J.* **1994**, *13*, 318-326.
5. R. D. Chavan, S. Bapat, V. Patil, A. Chowdhary, A. Kale, *Recept. Clin. Investig.* **2018**, *5*, 1-11.
6. P. Y. Child, **2013**.
7. D. M. Morens, J. K. Taubenberger, *Rev. Med. Virol.* **2011**, *21*, 262-284.
8. Z. Liu, J. Zhao, W. Li, X. Wang, J. Xu, J. Xie, K. Tao, L. Shen, R. Zhang, *Comput. Math. Methods Med.* **2015**, *2015*, 480764.
9. M. Abdullahi, G. A. Shallangwa, A. Uzairu, *Beni-Suef Univ. J. Basic Appl. Sci.* **2020**, *9*, 2.
10. K. Ide, Y. Kawasaki, K. Kawakami, H. Yamada, *Curr. Med. Chem.* **2016**, *23*, 4773-4783.
11. H. Patel, A. Kukol, *Drug Discov. Today* **2021**, *26*, 503-510.
12. A. Amir, M. Siddiqui, N. Kapoor, A. Arya, H. Kumar, *Trends Bioinform.* **2011**, *4*, 47-55.
13. V. K. Narayanaswamy, M. Rissdörfer, B. Odhav, *Int. J. Theor. Appl. Sci.* **2013**, *5*, 45-49.
14. L. Zhang, M. A. Williams, D. B. Mendel, P. A. Escarpe, X. Chen, K. -Y. Wang, B. J. Graves, G. Lawton; C. U. Kim, *Bioorg. Med. Chem. Lett.* **1999**, *9*, 1751-1756.
15. S. J. Clarke, T. L. Gilchrist, A. Lemos, T. G. Roberts, *Tetrahedron* **1991**, *47*, 5615-5624.
16. D. E. Arthur, B. O. Elegbe, A. O. Aroh, M. Soliman, *Bull. Natl. Res. Cent.* **2022**, *46*, 1-29.
17. M. Appell, J. Willett, F. A. Momany, *Carbohydr. Res.* **2005**, *340*, 459-468.
18. D. E. Arthur, J. N. Akoji, R. Sahnoun, G. C. Okafor, K. L. Abdullahi, S. A. Abdullahi, C. Mgbemena, *Bull. Natl. Res. Cent.* **2021**, *45*, 1-12.
19. S. Singh, M. J. Jedrzejas, G. M. Air, M. Luo, W. G. Laver, W. J. Brouillette, *J. Med. Chem.* **1995**, *38*, 3217-3225.
20. G. Šinko, *Chem. Biol. Interact.* **2019**, *308*, 216-223.
21. A. A. Naqvi, T. Mohammad, G. M. Hasan, M. Hassan, *Curr. Top. Med. Chem.* **2018**, *18*, 1755-1768.
22. R. Huey, G. M. Morris, S. Forli, *Scrapp. Res. Instit. Molecul. Graph. Lab.* **2012**, *10550*, 1000.
23. D. E. Arthur, *Radiol. Infect. Dis.* **2019**, *6*, 68-79.
24. M. Kumar, S. -M. Chung, G. Enkhtaivan, R. V. Patel, H.-S. Shin, B. M. Mistry, *Int. J. Mol. Sci.* **2021**, *22*, 2368.
25. D. E. Arthur, A. Uzairu, *J. King Saud Univ. Sci.* **2019**, *31*, 1151-1166.
26. A. Ahmad, M. R. Javed, A. Q. Rao, T. Husnain, *BMC Complement. Altern. Med.* **2016**, *16*, 1-8.